DTU Informatik
Institut for Informatik og Matematisk Modellering

Conditional Random fields for multispectral data analysis

Sara Sharifzadeh, Line Clemmensen, Bjarne Erbsøll
Department of Informatics and Mathematical Modelling, Technical University of Denmark, email: sarash@imm.dtu.dk

Introduction

Multispectral imaging has become a critical component of many applications such as medical research and food quality control.

In spectral imaging, supplementary spectral data are exploited together with spatial information to extract more complete features such as ingredients and chemical components.

On the other hand, CRF has also found many applications in medical image labeling recently. Due to their ability to capture arbitrary dependencies among observations in contrast to MRFs [1].

Conditional Random Fields (CRF)

CRF is formulated based on the undirected graphical model.

Let *G = (V,E)* be a graph with vertices *V* and edges *E*. In the graph *G*, vertices *V = (X ∪ Y)* with *X* (observation) and *Y* (label) as random variables. Edges *E* define how the distribution is conditioned and each edge connects a pair of nodes. Conditional independence is represented by a clique in the undirected graphical model. A clique is a subset of nodes that are fully connected in the graph.

Then *(X, Y)* is a conditional random field when conditioned on *X*, the random variable *Y* obeys the *Markov property*. The random field that is globally conditioned on the observation *X* has the form:

$$P(y|x) = \frac{1}{z}\left(-\left[\sum_{v\in V}\lambda\phi(y_v, X) + \sum_{\langle i,j\rangle\in E}\beta\psi(y_i, y_j, X)\right]\right) \quad (1)$$

where ϕ and ψ are the unary and pair wise potentials, respectively. The former indicates the relationship between a single label and its observation and the latter, is the interaction potential related to neighbors. Λ and β are weights. Z is a normalizing factor called the partition function. The general graphical representation of CRF is as follows:

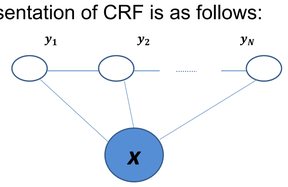

Figure 1. General graphical representation of CRF

CRF for Cell Classification

Recently, CRF has been used for classification and segmentation of sub-cellular structures [2,3]. Multispectral microscopy for applications in histology and cytology has shown that the unique transmission spectra of biological tissue provides additional information that improves the cell classification task. We would describe a cell classification task performed in [2].

Each 2D image pixel is classified as part of a cell or intercellular material. For spectral image sequences $X = (x_1, \dots x_M)$, is the observed vector and x_i is the spectral reflectance value acquired at a certain wavelength w_i with each $w_i \in [400nm - 700nm]$ with a spectral resolution of 10nm. The corresponding segmentation label is $Y = (y_1, \dots y_M)$ and $yi \in \{-1, 1\}$.

The posterior probability distribution of the segmentation **y** is modeled by three factors; 1) the local relationship between the observed data and the label; 2) spatial constraints along each edge in the 2D image; and 3) spectral constraints imposed by the label state in neighboring spectra. Considering the unary and pairwise clique potentials with the spectral constraints, the posterior distribution is expressed as a Gibbs distribution with the following form:

$$P(y|x) = \frac{1}{z}\exp(-[\boldsymbol{\Phi} + \boldsymbol{\Psi} + \boldsymbol{\Gamma}]) \quad (2)$$

where ϕ, ψ, Γ are defined as follows:

$$\boldsymbol{\Phi} = \sum_{v\in V,k}\lambda_k\phi_k(y_v, X) \quad (3)$$
$$\boldsymbol{\Psi} = \sum_{\langle i,j\rangle\in E,k}\beta_k\psi_k(y_i, y_j, X) \quad (4)$$
$$\boldsymbol{\Gamma} = \sum_{v\in V,k}\sum_{r\in N_v}\gamma_k\chi_k(y_{k,v}, y_{k-1,r}, y_{k+1,r}) \quad (5)$$

Where λ , β and γ are weights. k denotes the corresponding wavelength.

- The unary potential is modeled as a simple logistic regression classifier: $\phi(y_v, X) = \sigma(w^T x_i) = \frac{1}{1+\exp(-w^T x_i)}, i \in N_v \cup V, N_v$ is the number of spectral neighbors.
- Given the challenges of cytological smears, pairwise potentials $\boldsymbol{\Psi}$ is decomposed as: $\psi(y_i, y_j, X) = \psi^y(y_i, y_j)\psi^{y,x}(y_i, y_j, X)$ (7) ; where $\psi^y(y_i, y_j) = \begin{cases} 1-\alpha & if\ y_i = y_j \\ \alpha & otherwise \end{cases}, \psi^{y,x}(y_i, y_j) = \begin{cases} (1-\alpha)g_2(\nabla) & if\ y_i = y_j \\ \alpha g_1(\nabla) & otherwise \end{cases}$ where α is a constant near 1 which shows higher punishment if the adjacent labels are different and $g_1(\nabla) = \exp\left(-\frac{\nabla}{k}\right)^2, g_2(\nabla) = \exp(-\frac{k}{\nabla})^2$, where∇ indicates the strength of the edge. So the penalty goes up when the edge strength is high and labels are the same for neighbors or when the edge strength is low and labels are different.
- These rigid constraints, ignore the intensity changes between frames. Therefore, the mean intensity of each frame is calculated. Then, the mean value against the corresponding wavelength value is considered. Let $f(w)$ be the function of the spectral profile, then the spectral gradient $s(\nabla_{wi})$ at wavelength w_i is defined as $\frac{df}{dw}|_{w=w_i}$. This controls the strength of the relationship between spectral neighbors: $\chi(y_{k,v}y_{k-1,v}, y_{k+1,v}) = \frac{1}{s(\nabla_{wk})}\left(1-\delta(y_{k-1,v}, y_{k,v})\right) + \frac{1}{s(\nabla_{wk+1})}(1-\delta(y_{k,v}, y_{k+1,v}))$ (8)

If $s(\nabla_{wi})$ is small, then the label of the current frame is more likely to have the same labels as its spectral neighbors. CRF model is trained using the Maximum Likelihood and criterion loopy belief propagation (LBP) [4]. The LBP is also used for inference.

This CRF model is applied to the data from 12 smears. The result are satisfactory compared to watershed based method which is also used for cell classification.

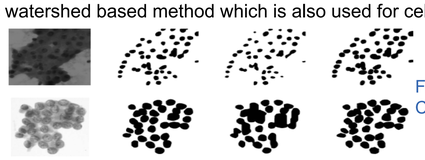

Figure 2.
Cell segmentation results

CRF for classification of milk acidification process

CRF can be used to classify the properties of acid milk gel into the state which best describes their rheological characteristics such as viscosity. The viscosity of acid milk increases during the acidification process [5].

At DTU Food laboratories, the sub-surface laser scattering (SLS) imaging experiments [6] have been performed during milk acidification process for CIFQ project. The feature vector, called log-log model, includes 22501 features per wavelength covering the whole acidification process. Totally, the SLS measurements have been performed in 116 different wavelengths ranging from 450nm -1020nm with the step size of 10 nm. Also the viscosity vector is calculated and has the same length of each feature vector 22501×1. The viscosity $\boldsymbol{Y}_{22501\times1}$, changes dramatically at gelation point corresponding to the conversion in milk gel structure (Figure 3.a). We consider this point to classify the feature vectors into two different states before and after gelation. The idea is to perform this classification using conditional random fields. Here, we show some pre-processes and the CRF model description as a suggestion for further studies.

As can be seen in figure 3.b, log-log features $\boldsymbol{X}_{22501\times116}$, do not change prominently in most wavelengths along the 22501 points of acidification. We have calculated the ratio of between-class to within-class variations univariately as follows:

$$score_{wn} = \frac{\sum_{c=1}^{2}|m_c - m|}{\sum_{c=1}^{2}\sum_{j=1}^{N_c}|x_{cj} - m_c|} \quad (9)$$

Where w_i denotes the n^{th} wavelength and m_c and m are the mean values of class c and total mean respectively. N_c is the number of training features in class c. The numerator shows the between class variations and the denominator is the within class variations. This score is calculated for all wavelengths and thresholded so that the 4 wavelengths with highest scores are chosen. Figure 4.a shows the variation profile of the 4 selected features as well as the scaled representation of their corresponding classes in dashed line.

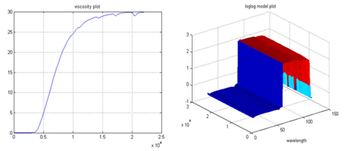

Figure 3. Viscosity and SLS log-log plots

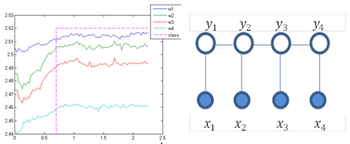

Figure 4. The features of selected wavelengths versus the state changes (left), proposed CRF (right)

It is clear that in each spectrum, a given SLS features value just depends on the physical scattering characteristic of acid milk in that wavelength. Therefore, the feature vectors at different wavelengths are independent to each other. However, the class labels in neighboring wavelengths are dependent since they describe the same sample. Thus, the posterior probability of the CRF model could be defined in the same way as in equation (2). The unary function Φ, describes the local dependencies of SLS features and classes using a logistic regression definition. The spatial pairwise penalty Ψ which models the similarity of spatially neighbor labels could be a function of gradient values of SLS features and the spectral constraints imposed by label state in neighboring spectra could be defined as a function of spectral gradient:

$$\psi^{y,x}\left(y_i, y_j\right) = \begin{cases} (1-\alpha)f(\frac{1}{\nabla_{x_i x_j}}) & if\ y_i = y_j \\ \alpha f\left(\nabla_{x_i x_j}\right) & otherwise \end{cases} \chi\left(y_{n,v}y_{n-1,v}, y_{n+1,v}\right) = f(\frac{1}{(\nabla_{wn})}, \frac{1}{(\nabla_{wn+1})}) \quad (10)$$

The graphical representation of such CRF model is represented in figure 4.b.

References:

1. Lafferty J., McCallum A., and Pereira F., ***Conditional random fields: Probabilistic models for segmenting and labeling sequence data***, International Conference on Machine Learning (ICML), 2001
2. Wu X. and Shah Sh. K., ***A Conditional Random Field Model for Cell Segmentation Using Multispectral Data,*** MICCAI Workshop on Optical Tissue Image analysis in Microscopy, Histopathology and Endoscopy Imperial College London September 24th 2009
3. Wu X. and Shah Sh. K., ***A Bottom-up and Top-down Model for Cell Segmentation using Multispectral Data,*** Proceedings of IEEE International Symposium on Biomedical Imaging, Rotterdam, The Netherlands, 2010.
4. Murphy, K., Weiss, Y., Jordan, M. ***Loopy belief propagation for approximate inference: an empirical study***, In Uncertainty in Artificial Intelligence 467–475 (1999).
5. Lucey A. J., Singh H. ***Formation and physical properties of acid milk gels: a review,***, Food Research Iniernational, Vol. 30, No. 7, pp. 529-542, 1998.
6. Nielsen O. H. A., Lindbjerg . Dahl A., Larsen R., Mller F., Donbk Nielsen F., Carsten L. Th. , Aans H. and Carstensen M.J., ***Supercontinuum Light sources for Hyperspectral ubsurface Laser Scattering Applications for Food Inspection,*** Scandinavian Conference on Image Analysis, Sweden , 2011